Open access • Journal Article • DOI:10.1061/(ASCE)BE.1943-5592.0000249

Analysis and Design of Straight and Skewed Slab Bridges

Patrick Théoret, Bruno Massicotte, David Conciatori

Institutions: École Polytechnique

Published on: 01 Mar 2012 - Journal of Bridge Engineering (American Society of Civil Engineers)

Topics: Bending moment, Slab and Shear force

Analysis and Design of Straight and Skewed Slab Bridges

Patrick Théoret[1]; Bruno Massicotte[2]; and David Conciatori[3]

Abstract: Results of an investigation aimed at determining bending moments and shear forces, required to design skewed concrete slab bridges using the equivalent-beam method are presented in this paper. Straight and skewed slab bridges were modeled using grillage and finite-element models to characterize their behavior under uniform and moving loads with the objective of determining the most appropriate modeling approach for design. A parametric study was carried out on 390 simply supported slabs with geometries covering one to four lane bridges of 3- to 20-m spans and with skew angles ranging from 0 to 60°. The analyses showed that nonorthogonal grillages satisfactorily predict the amplitude and the transverse distribution of longitudinal bending moments and shear forces, and can be used for the analysis of skewed slab bridges. Results of the parametric study indicated that shear forces and secondary bending moments increase with increasing skew angle while longitudinal bending moments diminish. Equations are proposed to include, as part of the equivalent-beam method for skew angles up to 60°, the increase of shear forces and the reduction of longitudinal bending moments. Equations are also given for computing secondary bending moments. A simplified approach aimed at determining the corner forces for straight and skewed bridges is proposed as an alternative to a more-refined analysis. The analyses indicated the presence of high vertical shear stresses in the vicinity of free edges that justifies suggesting to provide shear reinforcement along the slab free edges. DOI: 10.1061/(ASCE)BE.1943-5592.0000249.

CE Database subject headings: Skew bridges; Shear forces; Concrete slabs; Finite-element method; Design.

Author keywords: Bridges; Skew; Shear forces; Corner forces; Concrete slabs; Grillage model; Finite-element method.

Introduction

Solid slab bridges are common for short spans up to 25 m, whereas voided slabs or other structural systems are more economical for longer spans. Slab bridges are often encountered in rigid-frame systems and are used as wide beams on abutments and piers in simply supported or continuous structural systems, and they are an efficient structural system for short skewed crossings. Slabs that are on continuous support lines act as wide beams, and are reputed to be ductile and redundant structures. However, several questions were raised on the safety of solid concrete slabs following the collapse of Concorde Bridge in September 2006 in Laval, North of Montreal, which was caused by the failure of a deep cantilever solid slab supporting a dropping skewed span (Massicotte et al. 2007). The rupture was attributed to concrete degradation, which was caused by saltwater penetration over several years along an internal inclined plane, leaving an insufficient concrete area to carry the vertical forces. This eventually caused a shear failure, which could not be attributed, however, to insufficient shear strength if the concrete had been in good condition. Nevertheless, it resulted in a brittle shear failure with little warning, which in turn caused the death of five people and injury to six others. Therefore, the main concerns of the bridge authorities regarding solid concrete slabs can be summarized in the following questions: (1) What is the actual shear magnification at the obtuse corner for skewed bridges? (2) Can some load redistribution take place once local shear failure occurs and what are the conditions that can ensure load distribution? (3) Should solid slab bridges be reinforced for shear and, if so, up to what extent? The present paper primarily addresses the first question and provides some indications for the third one.

Very little attention has been paid to the analysis of skewed slab bridges, probably because they are generally perceived as one-way slabs in which the main longitudinal reinforcements carry the longitudinal moments, whereas secondary transverse reinforcements are determined by empirical rules. For skewed slab bridges, AASHTO (2007) recommends a reduction factor for bending moments, but no magnification factor for shear, as specified for other types of bridges, whereas Canadian Standards Association (CSA) (2006) imposes a limit for the use of the equivalent-beam method for skewed bridges without proposing any alternative beyond that limit. Finally, transverse and secondary moments can develop in skewed slab bridges, and no guidance on their magnitude is given in bridge codes. Menassa et al. (2007) concluded on the flexural behavior of skewed slabs that the decrease in longitudinal moments with a higher skew angle is offset by the transverse-moment increase. They recommend a three-dimensional finite-element analysis for skew angles beyond 20°.

Various degrees of refinements are possible in bridge analysis. Computers and software are constantly increasing the capabilities and ease for carrying out refined analysis. This may suggest that simplified analysis methods will progressively disappear. Such a conclusion is probably incorrect, but it is certainly undesirable. When possible, a refined analysis should be accompanied by

[1]Civil, Geological and Mining Engineering Dept., Ecole Polytechnique of Montréal, Station Centre-ville, Montreal, Québec H3C 3A7, Canada.

[2]Civil, Geological and Mining Engineering Dept., Ecole Polytechnique of Montréal, Station Centre-ville, Montreal, Québec H3C 3A7, Canada (corresponding author). E-mail: bruno.massicotte@polymtl.ca

[3]Civil, Geological and Mining Engineering Dept., Ecole Polytechnique of Montréal, Station Centre-ville, Montreal, Québec H3C 3A7, Canada.

simpler models. In bridges, the equivalent-beam method has been used since the 1930s (Zokaie et al. 1991), and is still used in North American bridge codes (AASHTO 2007; CSA 2006). This method, which should be on the conservative side, provides a simple and quick way to determine the load effects on the main supporting elements. Improving the accuracy while retaining the simplicity of the equivalent-beam method would contribute to maintaining its popularity and usefulness.

Grillage models are considered as refined method (CSA 2006) and would normally be the next step in analysis refinement after the equivalent-beam method. Common sense indicates that grillage models should remain simple for any type of bridges, and be limited to two-dimensional (2D) grids, in turn avoiding the complexity of pseudotridimensional modeling. Aside from their simplicity, grillage models generate information that is still manageable at the human level, but they also offer the advantage of giving load effects in members that can directly be linked to strength calculations that are specified in the codes. Although orthogonal grids are presented in the specialized literature (Hambly 1991; Jaeger and Bakht 1982), using nonorthogonal (or skewed) grids with members parallel to the slab sides greatly facilitates modeling. However, little information has been found in the literature on the appropriateness of this approach in the perspective of carrying out analysis for design. Ultimately, finite-element analysis would be the preferred finest modeling level. However, the more refined the model is, the higher the chances are of introducing errors. This is particularly true in specifying boundary conditions or introducing hinges for some bridge types. Moreover, finite-element models generate large amounts of data that can generally only be treated at the software level, which suggests greater attention. Stresses need to be integrated to obtain bending moments and shear forces, whereas in the case of concrete structures the load-effect components must be computed with respect to reinforcement orientation. For slab bridges, one should choose between plate elements or solid elements, the former being the natural choice. A gradual increase in analysis refinement is always a good practice. Because engineers would likely be more inclined to use the latest and most-efficient features that are offered by modern software, such an approach should be encouraged, and simplified methods such as the equivalent-beam analogy must be maintained in the codes.

This paper's objective is threefold. First, the paper was aimed at illustrating the behavior of straight and skewed solid slab bridges under uniform traffic loads by using the appropriate refined models with the goal of determining the maximum shear forces and bending moments in the context of a design or strength appraisal. The second objective was to derive a series of equations for the equivalent-beam method for considering the skew effects for longitudinal shear and bending moments, for both dead and live loads. The final objective was to develop a simple approach for determining the magnitude of secondary bending moments as a complement to the equivalent-beam method. The proposed simplified approach is developed to be used with either AASHTO (2007) or CSA (2006) specifications.

In the first part of the present paper, the behavior of straight and skewed slabs is examined in bending and shear, with the objective of determining the most-efficient grillage model between orthogonal and nonorthogonal arrangements, on the basis of a comparison against plate or solid finite-element model results. The second part of the paper presents the results of a parametric study on 390 solid slab bridges that served to derive equations for considering the skew effects in slab bridges when using the equivalent-beam method. Most bridges considered in this study were simply supported structures of one to four lanes, with spans L ranging from 3 to 20 m. The selected skew angles θ varied from 0 to 60°. Definitions are provided in Fig. 1.

Analysis for Design

Selected Refined Models

The behavior of solid slabs was studied by using four types of refined models: two grillage arrangements and two types of finite elements, as shown in Fig. 2. These models were selected with the objectives of comparing the advantages and limitations for each, and to identify the most appropriate in the context of design for bending and shear. Orthogonal-grillage models are recommended in various specialized publications (Hambly 1991; Jaeger and Bakht 1982). Although these models give load effects that can be handled more naturally for determining transverse moments, they bring limitations in setting the grid member spacing, which does not facilitate automating grid generation for skewed bridges. In contrast, nonorthogonal grillages with members parallel to the

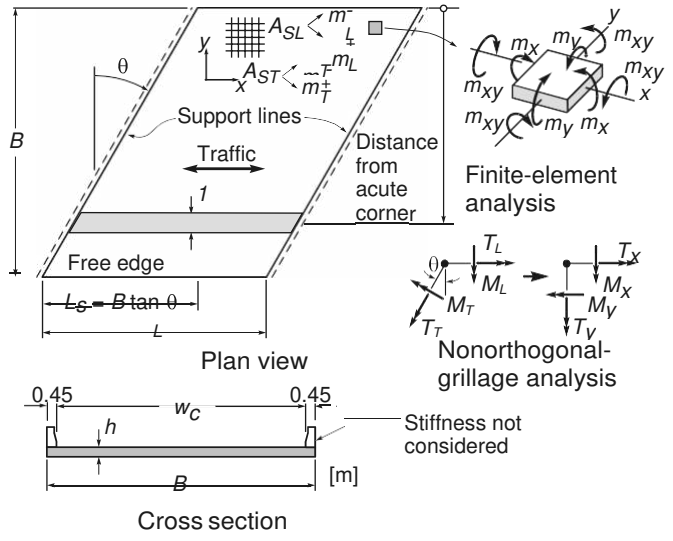

Fig. 1. Bridge geometry and bending-moment definitions

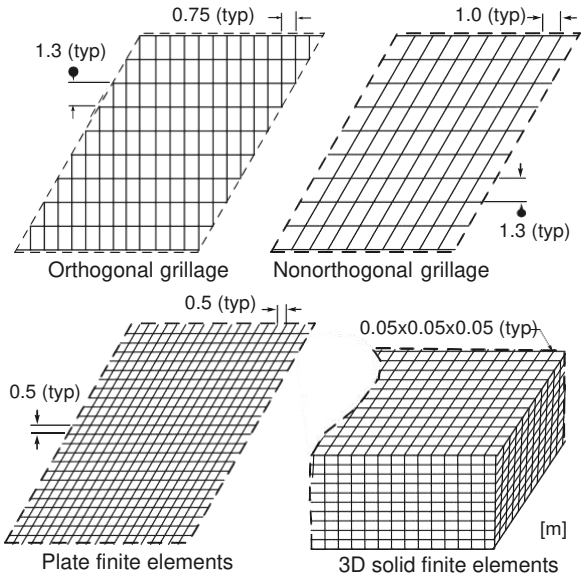

Fig. 2. Grillage and finite-element models

slab edges enable the generation of models without limitations in member spacing in both directions. However, little information is available on the accuracy of these models or how transverse moments can be treated. Plate elements would naturally be the preferred choice for slab bridges. However, near discontinuities such as the corners along the support lines, especially for skewed slabs, some plate elements can be susceptible to stress concentration or present limitations in the mesh refinement considering the slab thickness if a finer mesh is required. Finally, solid elements can very accurately represent the actual structures. However, the mesh-refinement level that is needed to obtain accurate results is often disproportioned for practical applications.

Design Bending Moments from Finite-Element Analysis

Determining flexural reinforcement from elastic finite-element bending moments requires including the contribution of the torsional moment. The following equations, obtained from equilibrium along axes parallel to the flexural cracks (Wight and MacGregor 2009), are used to evaluate the minimum positive and negative flexural resistances in the case of an orthogonal-reinforcement layout, in which the algebraic values of the bending moments per unit width are used:

$$m_L^{+} = m_x + |m_{xy}| \geq 0 \quad (1)$$

$$m_T = m_y + \frac{1}{\gamma}|m_{xy}| \geq 0 \quad (2)$$

$$m_L^{-} = m_x - |m_{xy}| \leq 0 \quad (3)$$

$$m_T^{-} = m_y - \frac{1}{\gamma}|m_{xy}| \leq 0 \quad (4)$$

As indicated in Fig. 1, m_x and m_y in these equations = longitudinal and transverse bending moments that are obtained in elastic analysis; m_{xy} = associated torsional moment; and m_L and m_T = bending moments that are required to design concrete slab reinforcement oriented in the longitudinal and transverse directions (A_{SL} and A_{ST} in Fig. 1), respectively. Codes conservatively specify $\gamma = 1$, but other positive values can be chosen freely (Nielsen 1999). Bending moments in the traffic (or longitudinal) direction for straight slab bridges are dominant, whereas torsional and transverse moments are negligible. However, for skewed bridge geometries, torsional and secondary moments, as given in Eqs. (2)–(4), can become important and require special attention as recommended by Menassa et al. (2007). Moreover, for concrete skewed bridges, longitudinal bending moments that are given by the equivalent-beam method must implicitly include the effect of torsion for designing reinforcement.

Design Bending Moments from Grillage Analysis

Two aspects require special considerations when modeling slabs with grillage models. First, the coupling of bending moments in each direction (M_X and M_Y in Fig. 1) associated with the Poisson's ratio cannot be reproduced in grillage models. Jaeger and Bakht (1982) proposed an approximate approach presented in the following equations, but, as they pointed out, the contribution of the transverse bending moment M_Y in the longitudinal direction is small and can be neglected:

$$M_{XC} = M_X + \upsilon M_Y \quad (5)$$

$$M_{YC} = M_Y + \upsilon M_X \quad (6)$$

where M_X and M_Y = bending moments obtained in grillage members parallel the x and y axes, respectively; and M_{XC} and M_{YC} = bending moments that approximately account for the coupling of orthogonal bending moments.

The second point is related to adopting nonorthogonal-grillage models as subsequently recommended in this paper. In this case, the flexural and torsional moments in the skewed transverse members (M_T and T_T) must be transformed in the x; y-axes system as follows if orthogonal reinforcements are used (Fig. 1):

$$M_Y = M_T \cos\theta + T_T \sin\theta \quad (7)$$

$$T_Y = -M_T \sin\theta + T_T \cos\theta \quad (8)$$

The bending and torsional moments per unit width (m_x, m_y, and m_{xy}) must then be computed by dividing the grillage member bending and torsional moments by the corresponding member spacing. Finally, the design moments required for determining the reinforcement are obtained using Eqs. (1)–(4) for orthogonal-reinforcement layouts.

Design for Shear

Shear strength has not been a concern for solid concrete slab bridges until recently with the collapse of the Concorde Bridge. Although shear stresses are generally small in slab bridges supported on continuous supports, closer attention should be paid to shear forces, especially at the obtuse corners of skewed bridges, but also in the presence of sidewalks and heavy parapets, or when discrete supports are used. For voided slab bridges that are analyzed as solid slabs, the design of webs for shear must correctly account for the effect of skew and the presence of sidewalks.

Limited information is available on the one-way shear strength of skewed slabs. Morrison and Weich (1987) carried out two large-scale tests on skewed slabs in which they measured high support reactions at the obtuse corner, as predicted by analysis. The failure was governed, however, by bending when using the typical flexural reinforcement ratio. They also observed shear-stress redistribution after shear cracking, which suggests that redistribution can take place in concrete slabs under certain conditions even without shear reinforcement. Sherwood et al. (2006) studied the shear behavior of wide beams and concluded that one-way shear strength is not affected by the beam width. Determining the critical shear sections would differ, depending on the load configuration, or if continuous or discrete supports are used. In the present study, simply supported continuous support conditions and a Poisson's ratio $\upsilon = 0.2$ were considered. These support conditions were chosen because they are representative of several existing structures, but also because the conclusions could be extended to single-span rigid-frame systems or structures supported on discrete supports.

Proposed Analytical Approach

Two approaches are proposed in this paper for designing skewed slabs. The first one uses the equivalent-beam method for determining the longitudinal bending moments and shear forces with correction factors to account for bending-moment reduction (C_M) and shear magnification (C_V) associated with the bridge skewed geometry. These factors were determined from a parametric study carried out using grillage analysis and are meant to be used with

AASHTO (2007) and CSA (2006) equivalent-beam methods. Along with these factors, a set of empirical equations are proposed for determining the secondary bending moments and the additional shear forces at the obtuse corner. These equations were obtained from plate and solid finite-element analyses.

The second approach consists of using grillage models for determining dead-load effects using Eqs. (1)–(8). However, as shown in the following section, the longitudinal bending moment (M_L) obtained using nonorthogonal-grillage layout for skewed bridge geometry (Fig. 1) can be directly used to compute the design bending moment in Eq. (1) using the following equation, where S_L = longitudinal grillage member spacing:

$$m_L = m_x \approx M_X/S_L = M_L/S_L \quad (9)$$

This approach avoids combining the concomitant bending and torsional moments caused by traffic loads as required in Eq. (1).

Flexural Behavior

Reference Bridge Geometry

The maximum longitudinal bending moments that are predicted by nonorthogonal-grillage models are first compared with those obtained by using orthogonal-grillage and finite-element plate models for two typical 10-m-long, 0.5-m-thick, 12-m-wide three-lane slab bridges with $\theta = 0°$ and $\theta = 30°$. The behavior of these structures was found to be typical of other slab bridges with a different geometry and is used in this paper to illustrate the characteristic responses of slab bridges. The results from a broader geometry spectrum are subsequently presented.

Both the orthogonal and nonorthogonal bridge models (Fig. 2) comprised 10 longitudinal members spaced at 1.3 m. For the nonorthogonal grillage, the transverse elements were spaced at 1.0 m, but transverse spacing for the orthogonal model was adjusted at approximately 0.75 m to accommodate the spacing of the supports along the longitudinal direction. The models were defined according to the rules presented in Appendix A. For the four-node plate shell elements adopted in the model (Fig. 2), the orthogonal plate dimensions were specified at 0.5 m. For the grillage models, rotations about an axis perpendicular to the support line were restrained, replicating the actual boundary conditions of continuous support lines. All the rotations were left free for the plate model because the vertical displacement restraint was sufficient to eliminate any rotation about an axis perpendicular to the support line. Not restraining the rotation as for the grillage model eliminated the need to include the support torsional moment for computing the reaction forces. Grillage and plate finite-element analyses were performed using SAP2000 [Computers & Structures, Inc. (CSI) 2009] software.

Bending Moments under Uniform Load

The results for a uniform load of 12 kN/m^2 corresponding to the slab self-weight are shown in Fig. 3. For all the models, the bending-moment values per unit slab width that were measured perpendicular to traffic (Fig. 1) are given along a line at midspan parallel to the supports. Finite-element longitudinal bending moments are given with and without consideration for the torsional moment (m_{xy}) as defined in Eq. (1). Orthogonal- and nonorthogonal-grillage model bending moments m_x were computed using Eq. (9).

As expected for the straight bridge in Fig. 3, all three models gave virtually the same results because of the absence of a torsional moment at midspan. The analysis showed the significant reduction

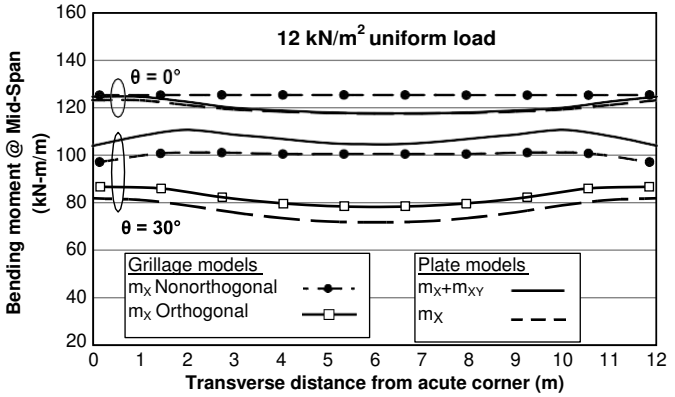

Fig. 3. Dead-load midspan bending moment for $L = 10$ m

of the longitudinal bending moments with the increase of the skew angle. For the skewed bridge, the design bending moment that was predicted by the nonorthogonal-grillage model compared very satisfactorily with the finite-element values for in which the torsional moments were considered according to Eq. (1). This illustrates the ability of nonorthogonal-grillage models to compute directly the bending moments that are required for concrete slab design without requiring any postprocessing for combining concomitant bending and torsional moments. This is explained by the fact that in nonorthogonal-grillage models, most of the load is being carried by the longitudinal grillage members, and the transverse torsional moment T_T is an order of magnitude smaller than M_Y of the orthogonal-grillage geometry. Conversely, the results obtained with the orthogonal-grillage model indicated that the design bending moments are not well captured when torsion is ignored. However, the magnitudes of all four moments in the orthogonal models were very close to the finite-element counterpart and are all of the same order of magnitude, which confirms the requirement of combining bending and torsional moments indicated in Eqs. (1)–(4).

Bending Moments under Truck Load

Fig. 4 illustrates the truck-load configurations used to compare the refined model predictions. The live load corresponds to CAN/CSA-S6-06 (2006) 625-kN five-axle truck loading that is defined in Fig. 4. The tire print sizes specified in CSA (2006) were used to apply the corresponding pressure in the finite-element model, whereas point loads on the members were used for the grillage models. Load configurations #1 and #2 approximately correspond to the governing load cases for flexure, whereas load configurations #3 and #4 were retained for shear according to the influence surface of the support reaction in the obtuse corner region. For configurations #3 and #4, the axle closest to the support was located at twice the slab thickness, which approximately corresponds to the governing condition giving the least shear strength for members without shear reinforcement (Wight and MacGregor 2009), as predicted by the general procedure in AASHTO (2007) in the case of tandem axle.

As shown in Fig. 5, the longitudinal bending-moment distributions at midspan (along line A-A) that were obtained by using the nonorthogonal grillage determined with Eq. (9) compare closely to the design moment distributions along the same line that were obtained with plate finite-element models using Eq. (1). Both shapes and amplitudes are well captured by the nonorthogonal models. Conversely, the bending-moment distribution obtained with the orthogonal model using Eq. (9) underestimates the

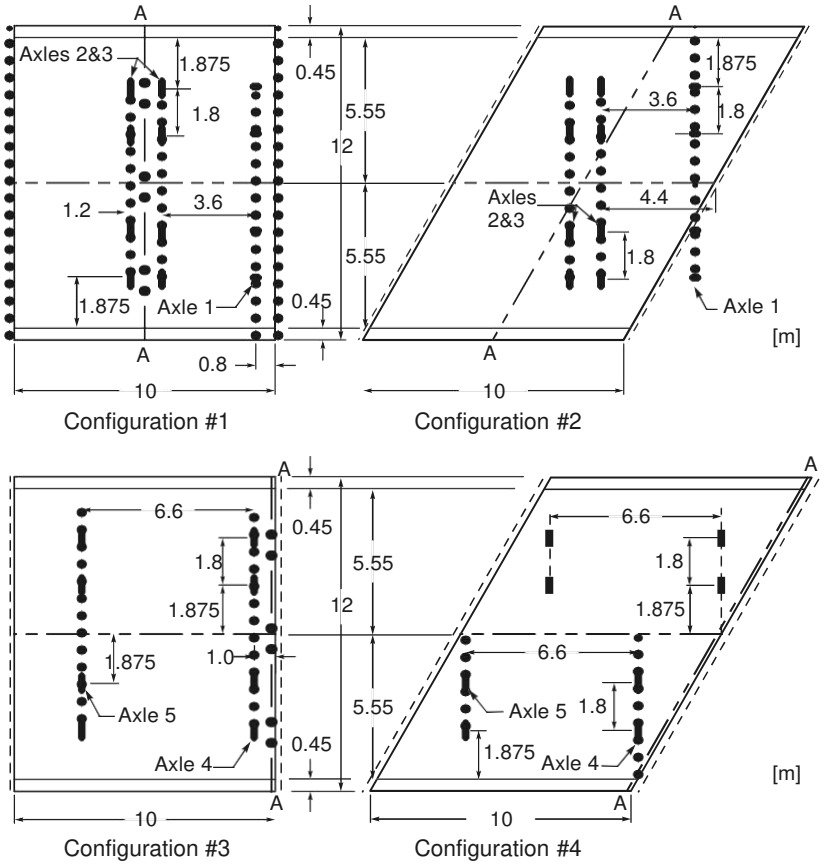

Note: CSA-S6 truck-load axles 1 to 5: 50-125-125-175-150kN @ 3.6-1.2-6.6-6.6 m
Tire foot print: 50-kN axle: 0.25x0.25m; other axles: 0.25x0.6m

Fig. 4. Truck-load configurations

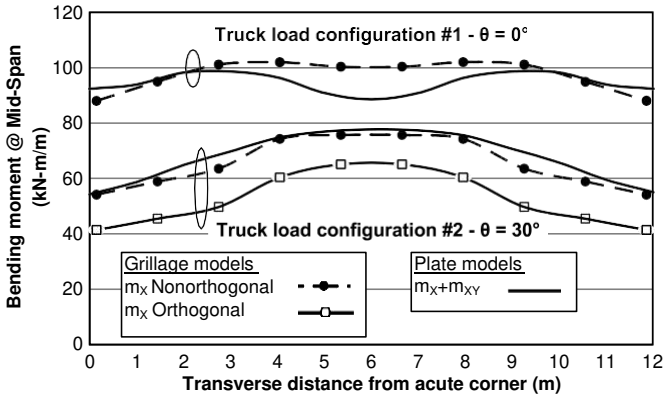

Fig. 5. Truck-load bending moment at midspan for L ¼ 10 m

amplitude of the design moment for skewed bridges when the torsion effects are not included.

Nonorthogonal-Grillage Validation

Analyses of a series of nonorthogonal-grillage and plate finite-element models were carried out to evaluate the accuracy of nonorthogonal grillages for determining the design bending moments for skewed bridges. Twenty 12-m-wide bridges with spans of 5, 10, 15, and 20 m were modeled as nonorthogonal grillages and plate finite elements for skew angles of 0, 15, 30, 45, and 60°. A constant span-to-thickness ratio (L=h) equal to 20 was used in all the models. The bridges were modeled with the same refinement as described previously. The maximum bending moments along a line at midspan parallel to the supports are compared for the case of a uniform load. Table 1 shows a grillage and finite-element model of the bending-moment ratios (m_G=m_{FE}) for three different conditions: (1) maximum bending moments ignoring torsional moments in the finite-element analysis ($m_{G\ max}$=$m_{X\ max}$), (2) maximum bending moments by using Eq. (1) for the finite-element results ($m_{G\ max}$=$m_{L\ max}$), and (3) comparison of the average bending moments for both models ($m_{G\text{Average}}$=$m_{L\text{Average}}$).

Globally, the comparison is acceptable with a ratio $m_{G\ max}$=$m_{L\ max}$ ¼ 1:0 when considering all the cases. All the bending moments obtained with the grillage model exceed the finite-element values when ignoring the torsion effects in processing finite-element results ($m_{G\ max}$ > $m_{X\ max}$). For θ¼0°, all the ratios are virtually equal to 1.0, whereas the grillage-model values for θ ⅙60° and L 5¼m are very conservative, and, therefore, the results for these cases will not be included in the following comparison because they are limit cases. On average for the 15 other cases, the maximum bending-moment values ($m_{G\ max}$) computed with the nonorthogonal-grillage model underestimated by 7% with a standard deviation of 6% of the corresponding finite-element values in which the torsional moment [$m_{L\ max}$ with Eq. (1)] were included. The flexural ductility of reinforced concrete slabs often justifies the consideration of the average moments over the slab

Table 1. Accuracy of Nonorthogonal-Grillage Models

L (m)	$m_G=m_{FE}$	θ ¼ 0°	θ ¼ 15°	θ ¼ 30°	θ ¼ 45°	θ ¼ 60°	Average
5	$m_G=m_{X\,max}$	1.04	1.10	1.35	1.82	2.97	1.66
	$m_{G\,max}=m_{L\,max}$	1.04	0.94	0.96	1.07	1.59	1.12
	$m_{Gavg}=m_{Lavg}$	1.15	1.05	1.07	1.28	2.07	1.33
10	$m_G=m_{X\,max}$	1.02	1.05	1.21	1.48	2.04	1.36
	$m_{G\,max}=m_{L\,max}$	1.02	0.89	0.90	0.97	1.16	0.99
	$m_{Gavg}=m_{Lavg}$	1.04	0.95	0.94	1.07	1.92	1.18
15	$m_G=m_{X\,max}$	1.01	1.06	1.19	1.46	1.73	1.29
	$m_{G\,max}=m_{L\,max}$	1.01	0.89	0.87	0.94	1.04	0.95
	$m_{Gavg}=m_{Lavg}$	1.03	0.94	0.91	1.38	1.26	1.10
20	$m_G=m_{X\,max}$	1.02	1.06	1.18	1.42	1.66	1.27
	$m_{G\,max}=m_{L\,max}$	1.02	0.89	0.86	0.88	1.00	0.93
	$m_{Gavg}=m_{Lavg}$	1.03	0.93	0.89	0.95	1.11	0.98
Average	$m_G=m_{X\,max}$	1.02	1.07	1.23	1.54	2.10	1.39
	$m_{G\,max}=m_{L\,max}$	1.02	0.90	0.90	0.97	1.20	1.00
	$m_{Gavg}=m_{Lavg}$	1.06	0.97	0.95	1.17	1.59	1.15

width at ultimate limit state as for the yield line analysis. In that case, the grillage models overestimated by 4% the finite-element values for all the cases considered in this comparison. It is noteworthy that the largest discrepancy occurs for θ¼ 30°, which is the skew angle that was purposely selected previously for illustrating the behavior of skewed slabs. The results of the θ¼ 30° and L ¼ 10 m case that are shown in Fig. 3 for a uniform load and in Fig. 5 for the truck load, illustrate the adequacy of nonorthogonal-grillage models to satisfactorily predict bending-moment amplitudes and distribution across the slab.

Analysis of the nonorthogonal-grillage model predictions for all the cases considered allows for the conclusion that it is the preferred approach for computing the longitudinal bending moments that are needed to design main flexural reinforcement. Its accuracy is comparable to the plate finite-element models without the associated complexity of combining the concomitant quantities m_x and m_{xy} according to Eq. (1). In addition, on the basis of these analyses, one concludes that orthogonal-grillage models are not appropriate for obtaining the required bending moments for the reinforcement design unless combining the concomitant quantities m_x and m_{xy} as for finite-element analysis, which makes its application less appealing. Finally, grillage models require postprocessing to determine the positive and negative transverse bending moments required to design the reinforcement [Eqs. (2) and (4), respectively]. Although this can be done relatively simply for dead load using Eqs. (7) and (8), this approach is not practical in the case of live load if these moments require an accurate evaluation.

Shear Forces

Plate Behavior

Simply supported straight plates that are subjected to uniform loading present additional reaction forces at the corners that are caused by a transverse curvature, which is a well-known phenomenon in plate theory (Timoshenko and Woinowsky-Krieger 1959). Fig. 6 illustrates the variation of the vertical reaction expressed as the ratio of the local reaction force divided by the average reaction for a 10-m-long and 12-m-wide bridge subjected to a uniform load that was analyzed by using finite-element plate elements. Results are given for normal and limit cases (e.g., zero Poisson's ratio and fixed rotation) to identify the governing parameters. For straight slabs, it can be observed that corner reactions gain in importance with increasing slab slenderness while it significantly reduces for fixed ends and vanishes for a zero Poisson's ratio or for restrained torsional rotation. For skewed bridges, corner reactions are important at the obtuse corner, with a magnification factor above 10 for the reference slab and nearly 9 with zero Poisson's ratio. However, this factor considerably reduces for fixed ends. Orthogonal- and nonorthogonal-grillage models for the skewed slab in Fig. 6 gave magnification factors of 2.52 and 1.36, respectively, very far from the 10.1 value obtained with the plate finite-element model.

Questions were raised regarding the actual magnitude and extent of the reaction forces at the corners. Further analyses of the same slabs with refined solid finite-elements carried out using ABAQUS (Hibbitt et al. 2009) with 10 50-mm-thick eight-node elements with reduced integration over the slab depth (see Fig. 2), showed that

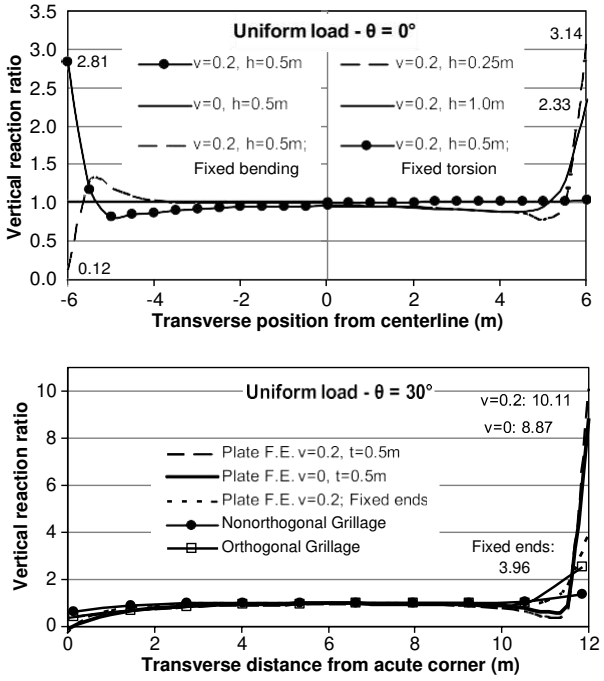

Fig. 6. Plate-element vertical reaction at support for a uniform load

stress concentrations at the supports are real with a magnitude less, but still close to those given by plate finite-element analysis (2.8 and 2.6 for the plate and solid finite-element models, respectively). However, a detailed examination of the shear-stress distribution in the case of a uniform load indicated a magnification factor that varied from 2.6 at the corner of a straight slab to nearly 1.0 at a distance equal to the slab thickness (h) when traveling along the corner diagonal. Moreover, the solid finite-element analyses pointed out the presence of additional vertical shear stresses along the slab free edges that vanish within a distance perpendicular to the side equal to the slab thickness. Fig. 7 shows the amplitude of the vertical shear stress measured in the slab longitudinal direction (from midspan to the support) along lines located at various distances from the slab free edge (0, 0.1 h, 0.5 h, and h). These results illustrate that the corner reaction force is not a local effect, but rather the accumulation of vertical shear forces that are induced by the transverse curvature. Even at sections away from the support line (e.g., at 2 h corresponding to 4 m in Fig. 7), the shear stress near the free edge is approximately twice the beam-theory value. Except with very refined models using solid finite-element, such as the one used in this study, these forces cannot be estimated. For solid slabs, the associated shear stresses are relatively small. However, when combined with a sidewalk or in the case of voided slabs, these shear forces need to be considered adequately. A closer look at these forces is presented afterward.

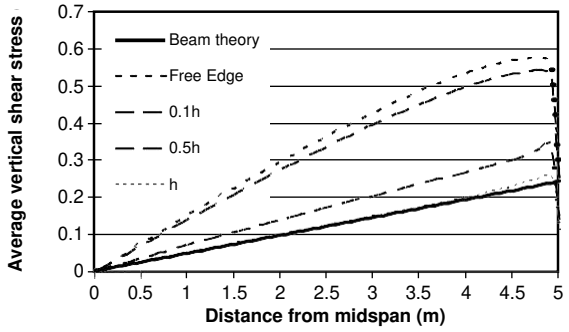

Fig. 7. Vertical shear stress along the free edge

Shear along the Support Lines at the Obtuse Corners

Fig. 8 shows the shear forces computed along the support line for the 10-m-long, 12-m-wide reference bridge for a uniform load of 12 kN=m^2 corresponding to the slab self-weight. The results are given per unit slab width measured perpendicular to traffic. Shear forces were obtained using solid finite-elements and the nonorthogonal-grillage model for two skew conditions: θ¼ 0° and θ ¼30°. Fig. 8 also shows the shear forces computed along the support line for the four truck-load configurations shown in Fig. 4 for the same two skew angles. These results show important corner forces for a straight bridge under a uniform load, but little effect in the case of truck load. In contrast in the case of skewed bridges, the corner reaction is significant for all the cases. However, the length along which support shear forces are affected is relatively small, typically equal to approximately the slab thickness. A close examination of the results suggests separating the localized corner effects to the rest of the support shear forces.

A comparison of the reaction forces in Fig. 8 between configurations #1 and #2 or configurations #3 and #4 indicates that increasing the skew angle changed the shape and amplitude of the shear-force distribution. The position of the shear-force peaks

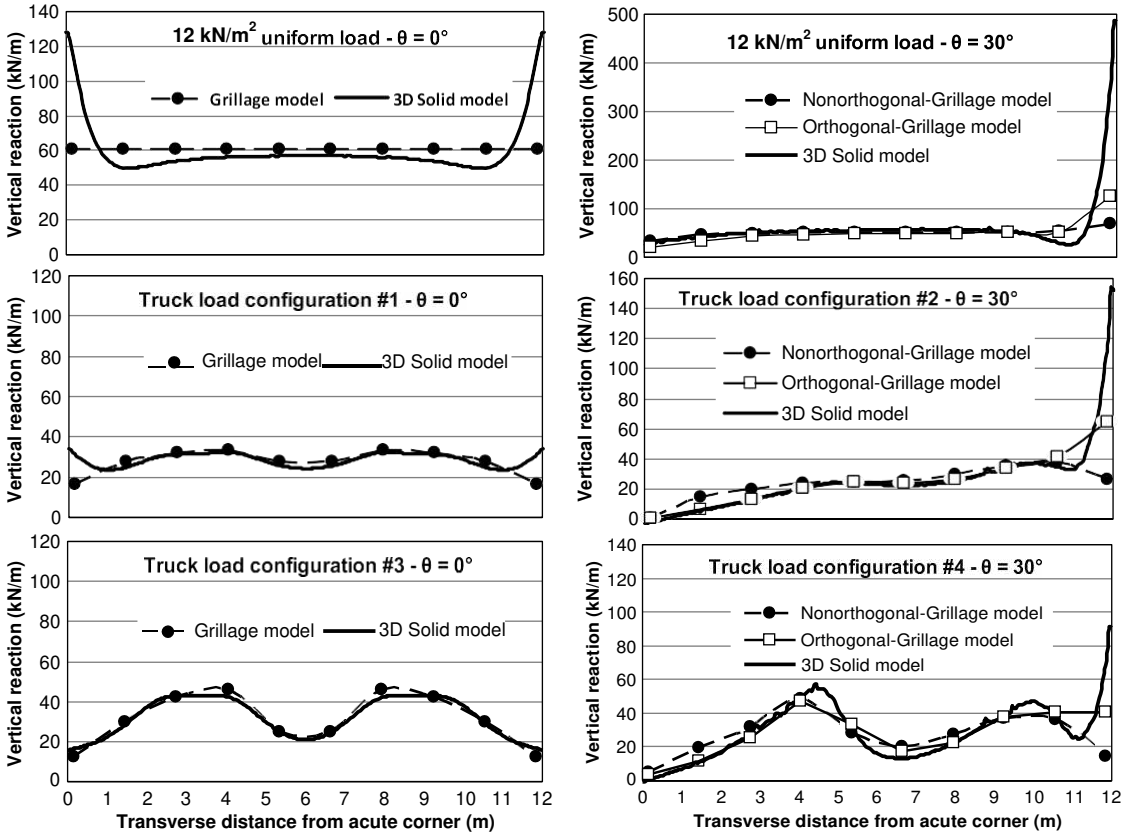

Fig. 8. Support vertical reaction for a 10-m-long bridge

moved toward the obtuse corner for the skewed bridges. Although the load conditions were not identical between straight and skewed geometries, and cannot be compared directly, these results allow interesting observations. First, the corner effects are virtually inexistent for straight bridges (configurations #1 and #3), whereas their contribution cannot be neglected for skewed geometry. Second, the shear forces associated to the remote axles (configurations #1 and #2) are distributed evenly over the support length, a phenomenon well captured by the grillage models. Finally, corner effects are more significant for the uniform load case for straight and skewed geometries. The analyses showed that nonorthogonal grillages satisfactorily predict the amplitude and the transverse-distribution shape of shear forces when compared with refined solid finite-element analysis, and, therefore, can be used confidently for the analysis of shear in skewed slab bridges, with the exception of the corner reactions.

Corner reactions must be considered separately because it would be inappropriate to use these forces to design slabs for shear over their full width, whereas simplified approaches such as the equivalent-beam method must predict the amplitude of the maximum shear forces for straight and skewed slabs across the entire slab width.

Corner Forces

Several parameters affect the amplitude of corner forces. Factors such as continuity, slab geometry, support configuration (continuous or discrete), support stiffness, cracking, and load configurations, just to name a few, should be considered. Although such an undertaking is beyond the scope of the study presented in the present paper, refined linear analyses contributed to illustrate the behavior. Observation of Figs. 6–8 results suggests that the amplification of the shear force near the corners originates from two distinct phenomenon: a first one attributed to bending and the associated transverse curvature, and a second one related to the skewed geometry. Fig. 9 illustrates for straight slabs ($\theta = 0°$) loaded uniformly that the maximum shear force at the slab corner increases almost linearly beyond the beam-theory level (vertical shear ratio equal to 1.0) with increasing aspect ratio B/L up to $B/L = 0.5$, and reaches a maximum value of approximately 2.0

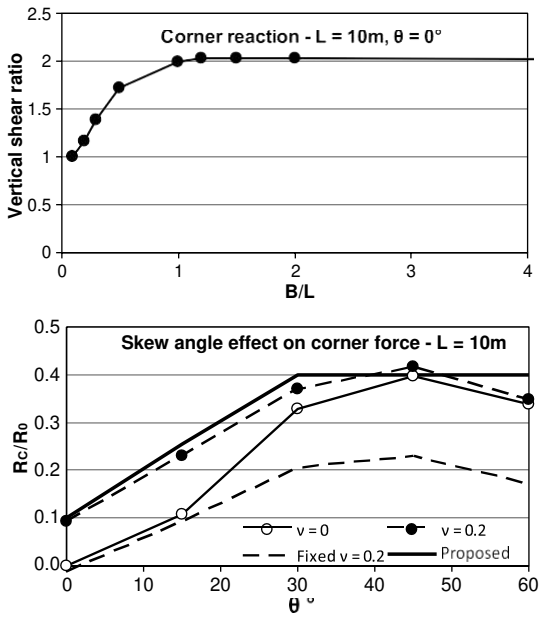

Fig. 9. Corner forces

for $B/L = 1:2$, with the case illustrated in Fig. 8. Results in Figs. 8 and 9 for skewed bridges clearly show that corner forces become more significant with larger skew angle. Conveniently, corner forces (R_C) are defined as the summation of the shear forces beyond the beam-theory shear-force level at the corners, and are equal to the contribution of the bending (R_B) and the skewed geometry (R_S) components. The magnitude of these forces is presented in the following as a function of R_0, the load applied to a quarter of the slab and defined as $R_0 = qBL/4$. The examination of the analysis results of simply supported slabs with $0.3 \le B/L \le 1.0$ under a uniform load indicates that $R_B = 0.1R_0$ for a Poisson's ratio of 0.2.

Solid finite-element analyses of slabs with span ranging from 5 to 20 m and for skew angle varying from 0° to 60° allowed capturing the value of effect of skew of the corner reactions. Fig. 9 illustrates the variation of the obtuse corner forces as a function skew angle for three conditions: simply supported, fixed against rotation at the supports, and simply supported with a Poisson's ratio equal to zero. This later condition is aimed at illustrating a limit case that could exist for example with extensive cracking. For the reference slab (simply supported and $\nu = 0.2$), R_C/R_0 is equal to 0.1 for $\theta = 0°$ and increases almost linearly up to 30°. The same trend was obtained for the fixed conditions, but values are less than half those of the simple slab. The condition with $\nu = 0$ illustrates that important reaction forces can be obtained for large skew angles without any coupling between longitudinal and transverse bending. Results for span between 5 and 20 m were identical to those obtained for the 10-m slab presented in Fig. 9.

Finally, the analyses indicated that corner forces associated with skewed geometry become important for skew angle beyond 20° and that 40% of gravity loads are concentrated at corners for $\theta \ge 30°$ for simply supported slabs and half this value for fixed conditions.

Analysis of Skewed Slabs Using the Equivalent-Beam Method

Current Code Specifications and Limitations

For skewed slab bridges, AASHTO (2007) recommends a reduction $r = 1.05 - 0.25 \tan\theta \le 1$ factor for bending moments, but no indications are provided to consider shear magnification attributable to skew, as specified for other types of bridges. CSA (2006) does not specify any correction factors for shear or bending moment, but rather imposes a maximum limit of 1/6 to the parameter $\varepsilon = B/L \tan\theta$ for using the equivalent-beam method for skewed bridges, where ε corresponds to the ratio of the slab width B projected in the longitudinal direction (L_S) to the span length L (see Fig. 1).

No indications are given in any codes for specifying transverse and secondary reinforcements. For this reason, Menassa et al. (2007) recommended limiting the application of the equivalent-beam method to 20° skewed bridges. Their study also indicated that the reduction factor r is appropriate for a short span (7.2 m), but it is overly conservative for longer spans (16.2 m). Codes would benefit, therefore, from clearer specifications on several aspects regarding skewed slab design that is associated with the equivalent-beam method, particularly for shear, moment reduction, and secondary reinforcements, as considered in the next sections.

Parametric Study

An extensive parametric study was performed on straight and skewed slab bridges for determining the effects of the geometrical

bridge characteristics on bending moments and shear forces caused by dead and live loads.

Slab bridges were selected to cover the most common geometries encountered in highways. Only simply supported bridges with simple spans ranging from 3 to 20 m were selected because it was assumed that the skew effects would be less important for continuous bridges as indicated by the results presented previously. The width was varied from 6.9 to 17.9 m, covering one to four lane bridges. The slab thickness h was assumed equal to L=20. Three different lane widths were considered for each bridge type (narrow, normal, and wide) to account for lane-width variation in determining the critical cases for live-load distribution. For each skew angle, a total of 78 bridge geometries were determined, whereas five skew angles were studied, from 0 to 60° by increments of 15°, for a total of 390 grillage models. Nonorthogonal-grillage models were used because they definitely appear to be the most optimal modeling approach to obtain the design bending moments and shear. CSA (2006) 625-kN five-axle truck model defined in Fig. 4 was applied using the software SAP2000 (CSI 2009) for all the possible configurations of the lane number and transverse truck position.

Shear Magnification

For each of the 78 bridge configurations, the skew effects were obtained by comparing the values of the skewed bridges with those of the corresponding straight bridge. Such comparison is, therefore, independent of the type of truck-load model and would therefore apply to both AASHTO (2007) and CSA (2006) truck models. The ratios of the maximum bending moment and shear in skewed bridges to the corresponding straight bridge values were computed for each of the 312 skewed bridges, expressed as follows:

$$C_V = V_{\theta>0}/V_{\theta=0} \quad (10)$$

$$C_M = M_{\theta>0}/M_{\theta=0} \quad (11)$$

A comparison of the parametric study values to the CAN/CSA-S6-06 parameter ε is shown in Fig. 10 for dead and live loads. The results clearly indicate that there is no definite tendency as a function of this parameter, but also that the ε=1=6 limit validity seems inappropriate. A closer examination of the results indicated that several of the bridges that are found under that limit are of common geometry, with spans between 10 and 20 m and a skew angle as small as 15°. This observation leads to the conclusion that the parameter ε is not adequate to characterize the shear magnification factor C_V in the case of skewed slab bridges.

The observation of the influenced surface for the obtuse corner reaction as illustrated in Fig. 11 revealed that part of the shear amplification factor observed in the grillage models is related to the ratio of the triangular surface originating from the obtuse corner over the total surface of the bridge, expressed as.

$$\beta = (L/B)\sin\theta\cos\theta \quad (12)$$

Fig. 12 shows the variation of C_V as a function of β and the number of lanes for dead and live loads. It is shown that the magnification factor can be as high as 2.0 in some cases, and is equal on average to 1.37 and 1.19 for dead and live loads, respectively. Two sets of equations are proposed to determine C_V for dead (C_{VD}) and live loads (C_{VL}) with the equivalent-beam method. The first one gives the best fit for the analytical results, whereas the second one is for a 95% confidence interval.

Best fit.

$$C_{VD} = 1 + (0.085B + 0.15)\beta \quad (13)$$

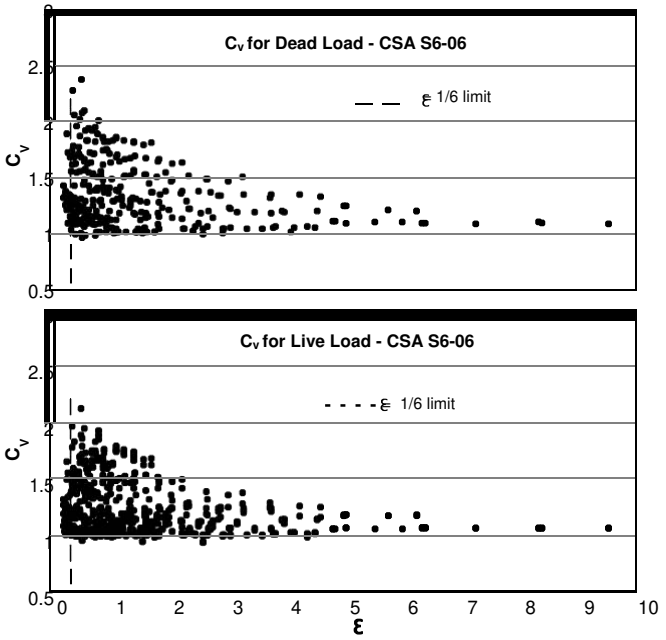

Fig. 10. CAN/CSA-S6-06 skew parameter

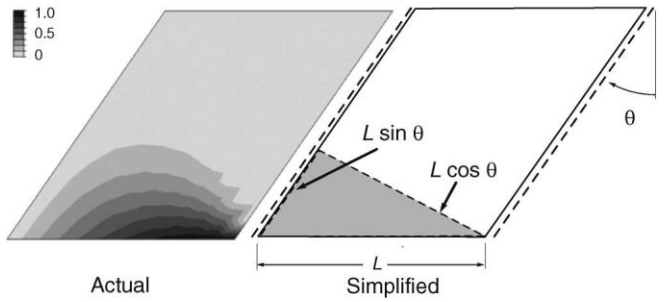

Fig. 11. Influence surfaces for obtuse corner reaction

$$C_{VL} = 1 + (0.075B - 0.15)\beta \quad (14)$$

with 95% confidence interval.

$$C_{VD95\%} = 1 + (0.095B + 0.25)\beta \quad (15)$$

$$C_{VL95\%} = 1 + (0.095B - 0.125)\beta \quad (16)$$

Fig. 12 also shows the ratio of the proposed equations to the analysis for the 95% confidence interval. The average values are equal to 1.09 and 1.12 for dead and live loads, respectively, with corresponding standard deviations of 6.67 and 8.57%. The proposed equations provide satisfactory results.

Moment Reduction

Fig. 13 presents the bending-moment reduction factor C_M that is given in Eq. (13) (or r in AASHTO) as a function of parameter β that is expressed in Eq. (12). The tendency for dead loads is clearly dependent on the skew angle and independent from parameter β. For live loads, C_M varies with the skew angle and parameter β. Closer study of the analysis results leads to the conclusion that the amplitudes of the bending moments in a skewed slab

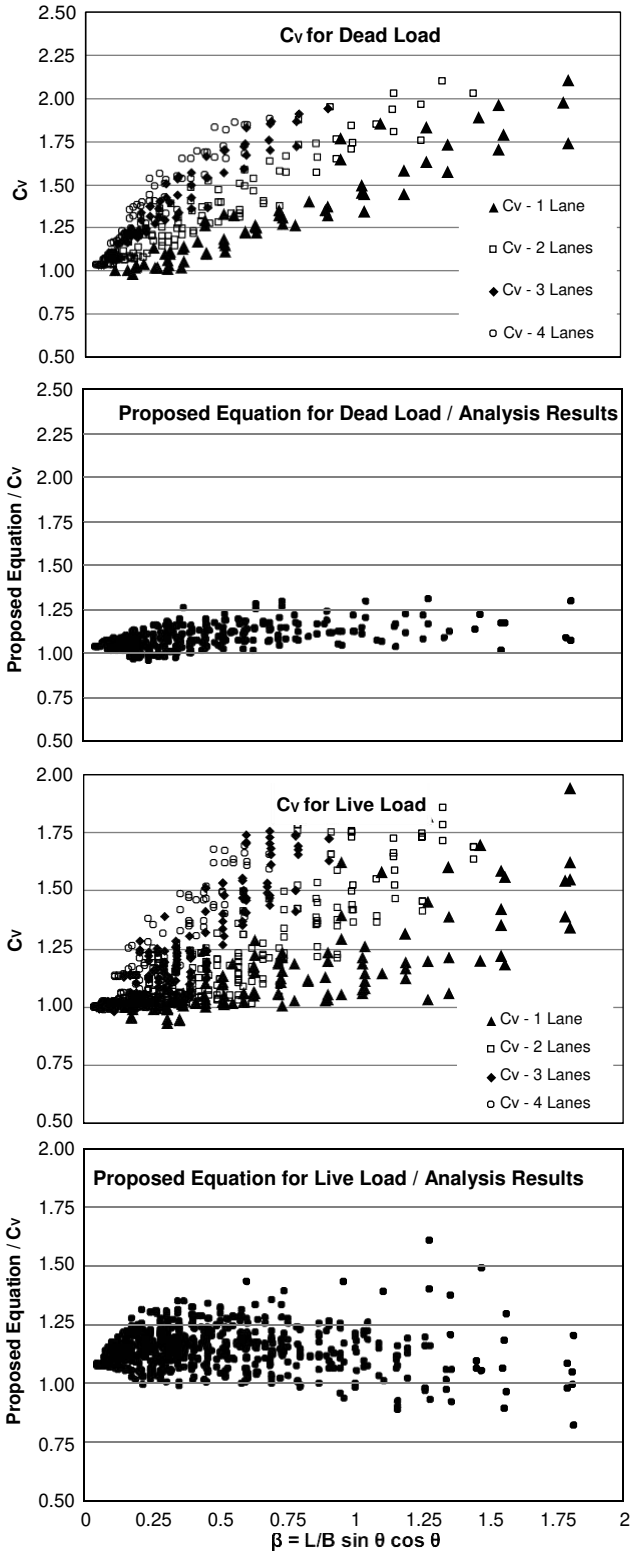

Fig. 12. Skewed bridge shear magnification factor

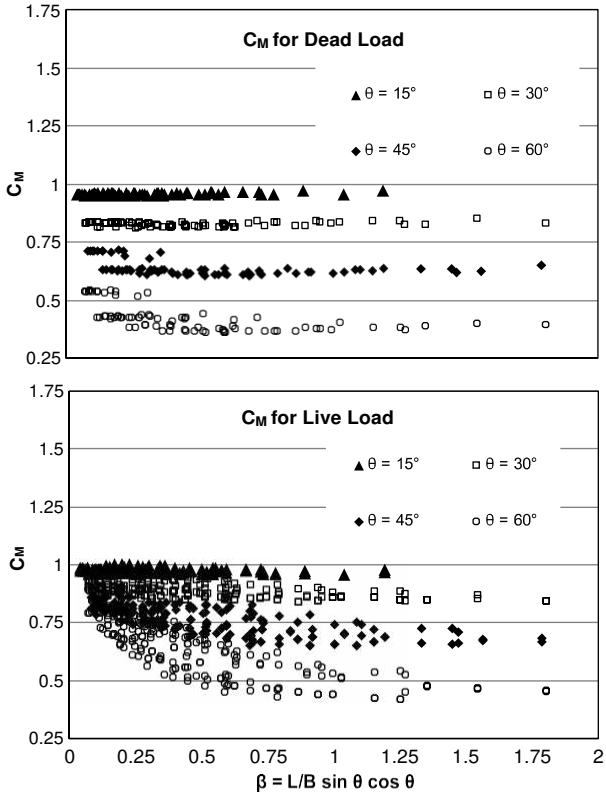

Fig. 13. Skewed bridge moment reduction factor

are directly related to the ratio of the span perpendicular to support edges. Two sets of equations are proposed to determine C_M for dead and live loads with the equivalent-beam method. The first one gives the best fit for the analytical results, whereas the second one is on the conservative side for 95% confidence interval. Although the analyses were carried out using CSA (2006) loading, results presented the same trend expressed in AASHTO (2007) recommendations given in Eq. (18). This observation supports the assumption made that the proposed equations are relatively independent of the live-load model for bridges with short to medium spans for which critical effects are obtained with concentrated loads.

Best fit.

$$C_{MD} = 1{:}05 - 0{:}28 \tan\theta \qquad (17)$$

$$C_{ML} = 1{:}05 - 0{:}25 \tan\theta \qquad (18)$$

With 95% confidence interval.

$$C_{MD95\%} = 1{:}05 - 0{:}335 \tan\theta \qquad (19)$$

$$C_{ML95\%} = 1{:}05 - 0{:}16 \tan\theta \qquad (20)$$

The average values given by the proposed equations to the analysis for the 95% confidence interval prediction are equal to 1.09 and 1.15 for dead and live loads, respectively, with corresponding standard deviations of 8.54 and 8.83%. From the results of the parametric study, the equation proposed by AASHTO for live load provides satisfactory results for a small skew angle and is increasingly conservative as the skew angle becomes larger.

Secondary Bending Moments

The effects of torsion are negligible on straight slab bridges, and transverse reinforcement design is governed by other requirements, such as minimum reinforcement limits. In the case of skewed slab bridges, torsion induces transverse and negative moments that cannot be neglected.

In the present study, the results of the finite plate element models on 20 bridges described previously were used to compare the secondary moments, obtained with Eqs. (2)–(4), to the maximum main longitudinal bending moments given by Eq. (1). Limited truck-load cases were also considered. Although the scope of this study is limited, clear tendencies were observed as shown in Fig. 14 in which the maximum value of each secondary moment is compared with the maximum longitudinal moment. The proposed relationships were kept on the safe side because of the limited number of cases considered.

$$m_L^- = m_L^+(-0.14 + \sin\theta) \geq 0 \quad (21)$$

$$m_T^+ = m_L^+(0.2 + \sin\theta) \quad (22)$$

$$m_T^- = m_L^+(0.1 + 0.4\sin\theta) \quad (23)$$

All of the secondary moments increase in amplitude with increasing skew angle. The longitudinal negative bending moments are negligible for a skew angle up to 10°, and can become as important as the longitudinal moments attributable to the torsion effects for a 60° skew angle. Eq. (21), as plotted in Fig. 14, is on the conservative side. Transverse positive bending-moment ratios start at 0.2 for a straight bridge, which are compatible with the adopted Poisson's ratio, and increase to 1.0 of a 60° skew angle, which complies with the Menassa et al. (2007) conclusions. Negative transverse bending moments are approximately half the positive-moment values as shown in Fig. 14 and as expressed in Eqs. (22) and (23). The ratios for the truck-load cases considered were less than the uniform load values and are below the values given by Eqs. (21)–(23).

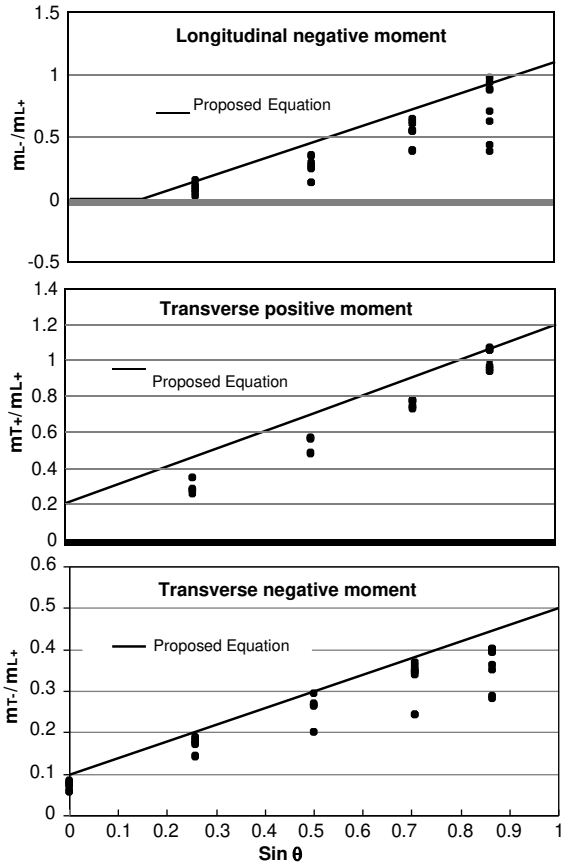

Fig. 14. Secondary moments

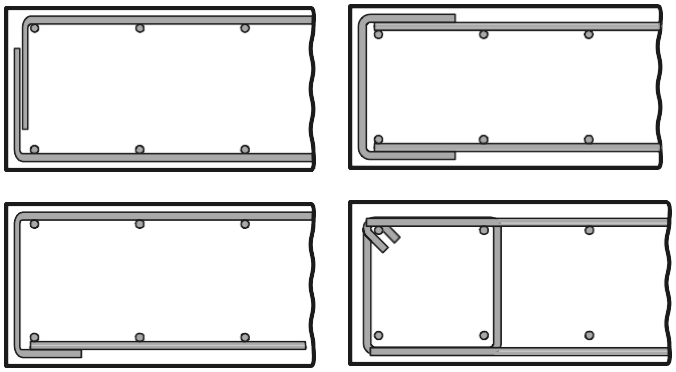

Fig. 15. Suggested shear reinforcement along free edges

The bending moments given by these equations, presented as positive quantities, are meant to be used with the equivalent-beam method. Other code requirements, such as minimum reinforcement, must also be used in parallel.

Corner Forces and Support Reactions

The solid finite-element analysis results allowed quantifying the two corner-force components identified previously as a function of geometrical parameters. These equations were derived for a uniform load for spans ranging from 5 to 20 m, with $0{:}1 \leq B/L \leq 1{:}4$ and $L/h = 20$. At obtuse corners, the total force is equal to $R_C = R_B + R_S$ (Fig. 9), whereas at acute corners the reaction force is equal to $R_B - R_S$, where

$$R_B = 0.5\sqrt{B/LR_0} \quad (24)$$

$$R_S = 0.6R_0\sin\theta \leq 0.3R_0 \quad (25)$$

In these equations, B should not be assumed greater L ($B/L \leq 1{:}0$ and $R_0 = qBL/4 \leq qL^2/4$). The values obtained with these equations may be reduced by half for fully fixed conditions. The uniform support reactions can be obtained by subtracting the corner forces to the total reaction force. In the case of discrete supports, the corner force must be attributed to the outermost supports, whereas it can be assumed that the remaining load is equally supported by the interior supports.

Free-Edge Reinforcement

The analyses reported in the present paper clearly indicate that important, but rather localized, shear forces develop along slab free edges, for straight and skewed geometries. As indicated previously, the shear forces in most of the slab area are not affected by these local effects. Fig. 15 presents suggestions for providing reinforcement details along the edges with the objective of providing some shear ductility. Similar reinforcement details were suggested by Morrison and Weich (1987) for skewed slab bridges, and by Nielsen (1999).

Summary and Conclusions

The paper presented the results of an investigation aimed at determining the bending moments and shear forces required to design skewed concrete slab bridges using the equivalent-beam method. Straight and skewed slab bridges were modeled using grillage and finite-element models to characterize their behavior under uniform and moving loads with the objective of determining the most appropriate modeling approach for design. A parametric study

was carried out on 390 simply supported slabs with geometries covering one to four lane bridges of 3- to 20-m spans and with skew angles ranging from 0 to 60°.

Comparison of finite-element analyses with grillage models suggested that nonorthogonal grid arrangements are preferred over orthogonal grillages. Not only are nonorthogonal arrangements simpler to realize than orthogonal grid models for skewed geometries, but their accuracy was found comparable to finite-element plate model values for determining the longitudinal bending moments in skewed slab bridges. In orthogonal-grillage and finite-element analysis, concomitant flexural and torsional moments for moving loads must be combined for determining the bending moments required for designing reinforcements which was found unnecessary with skewed grillage models in the longitudinal direction. Finally, all grillage and finite-element models require postprocessing to correctly predict the transverse bending moments using concomitant flexural and torsional moments.

Finite-element analyses confirmed that important reaction forces develop at slab corners. Theses forces are caused by the combination of transverse curvature and skew effects. Refined solid finite-element analyses indicated that the corner forces are related to additional vertical shear forces along the slab free edges that are present in a band equal to the slab thickness. It was concluded that corner reactions must be considered separately to beam shear because it would be inappropriate to use these forces with the equivalent-beam method to design for shear over the slab width. In that perspective, a simplified and conservative approach aimed at determining the corner forces for straight and skewed bridges was presented as an alternative to a more refined analysis. Recommendations for shear-reinforcement details along slab edges were also proposed to enhance the behavior of slab bridges in shear.

At the exception of the corner reactions, the analyses showed that nonorthogonal grillages satisfactorily predict the amplitude and the transverse distribution of shear forces along the support lines when compared with the refined solid finite-element analysis, and can therefore be used confidently for the analysis of shear in skewed slab bridges. The shear forces obtained with orthogonal grillages also compared satisfactorily with the finite-element values, but were not better than the nonorthogonal-grillage values to obtain the corner forces.

The results of a parametric study carried out on 390 slab bridges indicated that the shear forces and the secondary bending moments increase with increasing skew angle while longitudinal bending moments diminish. The study allowed proposing equations to consider the increase in shear forces attributed to skewed slab geometries to be used with the equivalent-beam method. The study also showed that the moment reduction factor in AASHTO is accurate for skew angles of up to 30°, but becomes very conservative for larger skew angles. Finally, equations for computing the secondary bending moments as part of the equivalent-beam method were proposed for slab bridges.

Equations and recommendations presented in this paper would allow to safely design slab bridges using the equivalent-beam method for bending moments and shear for skew angles up to 60°, for bridge with one to four lanes with spans up to 20 m. These equations are compatible with AASHTO (2007) and CSA (2006) for the ranges of parameters considered in this study. If more refined analyses are required, nonorthogonal-grillage models would be the preferred refined method for computing live-load longitudinal bending moments and shear forces. Plate finite-element models are suitable to evaluate secondary bending moments, but are not appropriate to determine the maximum amplitude of the reaction forces near support corners. However, the average amplitude of the reaction force obtained along a distance from the slab corner equal to the slab thickness conveys reasonable values. Finally, the use of shear reinforcement is recommended along the slab free edges.

Appendix. Grillage Modeling

Grillage layout and properties were determined according to Hambly (1991) recommendations. The maximum spacing of longitudinal grid element was measured as half the truck width for internal grid elements (3:0=2¼ ±1:5 m) and this value plus the curb width for external grid elements±(1þ5 0:45≈2 m). Maximum longitudinal grid-element spacing was measured less than one quarter of the bridge span. Beams at exterior edges were placed at a distance of 0:3*h* of the slab side, where *h* is the slab thickness. Member spacing in both directions should be similar when possible. For simplifying the modeling process with different bridge geometries, a fixed spacing of 1 m between transverse elements was used. This value is relatively close and generally smaller than the selected longitudinal grid spacing. It also simplifies the automation of grid model generation.

The two required member properties are.

$$J ¼ bh^3=6 \quad \text{ð26Þ}$$

$$I ¼ bh^3=12ð1 - v^2Þ \quad \text{ð27Þ}$$

where b = slab width associated to a given member; and h = slab thickness. For nonorthogonal grillage, b = width measured perpendicular to the member orientation.

Acknowledgments

The authors would like to acknowledge the financial support obtained from the Natural Sciences and Engineering Council of Canada, the Quebec Ministry of Transportation, and the Consultants Cimaþ of Montreal, Canada.

References

AASHTO. (2007). *LRFD bridge design specifications*, 4th Ed., AASHTO, Washington D.C.

Canadian Standards Association (CSA). (2006). "Canadian highway bridge design code." *CAN/CSA-S6-06*, Mississauga, ON, Canada.

Computers & Structures, Inc. (CSI). (2009). SAP2000-Integrated software for structural analysis and design. *Computers and Structures*, Berkeley, CA.

Hambly, E. C. (1991). *Bridge deck behavior*, E & FN Spon, New York.

Hibbitt, H. D., Karlson, B. I., and Sorensen, E. P. (2009). *ABAQUS version 6.8-3, finite-element program*, Hibbitt, Karlson & Sorensen, Providence, RI.

Jaeger, L. G., and Bakht, B. (1982). "The grillage analogy in bridge analysis." *Can. J. Civ. Eng.*, 9(2), 224–235.

Massicotte, B., Tremblay, R., Ghali, A., Grenier, J., and Blouin, B. (2007). "Study on the causes of Concorde Boulevard bridge collapse." *Rep. CDT-ST07-11*, Ecole Polytechnique of Montreal, Quebec, Canada (in French).

Menassa, C., Mabsout, M., Tarhini, K., and Frederick, G. (2007). "Influence of skew angle on reinforced concrete slab bridges." *J. Bridge Eng.*, 12(2), 205–214.

Morrison, D. G., and Weich, G. R. (1987). "Free-edge and obtuse-corner shear in reinforced concrete skew bridge decks." *ACI Struct. J.*, 84(1), 3–9.

Nielsen, M. P. (1999). *Limit analysis and concrete plasticity*, CRC Press, New York.

Sherwood, E. G., Lubell, A. S., Bentz, E. C., and Collins, M. P. (2006). "One-way shear strength of thick slabs and wide beams." *ACI Struct. J.*, 103(6), 794–802.

Timoshenko, S., and Woinowsky-Krieger, S. (1959). *Theory of plates and shells*, 2nd Ed., McGraw-Hill, New York.

Wight, J. K., and MacGregor, J. G. (2009). *Reinforced concrete: Mechanics and design*, 5th Ed., Prentice Hall, Upper Saddle River, NJ.

Zokaie, T., Imbsen, R. A., and Osterkamp, T. A. (1991). "Distribution of wheel loads on highway bridges." *NCHRP 12-26/1 Final Rep.*, National Cooperative Highway Research Program, Washington, D.C.